

# Real-Time Finite Element Monitoring of Sub-Dermal Tissue Stresses in Individuals with Spinal Cord Injury: Toward Prevention of Pressure Ulcers

ERAN LINDER-GANZ,<sup>1</sup> GILAD YARNITZKY,<sup>1</sup> ZIVA YIZHAR,<sup>2</sup> ITZHAK SIEV-NER,<sup>3</sup> and AMIT GEFEN<sup>1</sup>

<sup>1</sup>Department of Biomedical Engineering, Faculty of Engineering, Tel Aviv University, Tel Aviv 69978, Israel; <sup>2</sup>Department of Physical Therapy, Tel Aviv University, Tel Aviv, Israel; and <sup>3</sup>Department of Orthopedic Rehabilitation, Chaim Sheba Medical Center, Tel Hashomer, Israel

(Received 18 June 2008; accepted 17 November 2008; published online 25 November 2008)

**Abstract**—Patients with a spinal cord injury (SCI) are susceptible to deep tissue injury (DTI), a necrosis in excessively deformed muscle tissue overlying bony prominences, which, in wheelchair users, typically occurs in the gluteus muscles under the ischial tuberosities. Recently, we developed a generic real-time, subject-specific finite element (FE) modeling method to provide monitoring of mechanical conditions in deep tissues deformed between bony prominences and external surfaces. We previously employed this method to study internal tissue loads in plantar tissues of the foot [Yarnitzky, G., Z. Yizhar, and A. Gefen. *J. Biomech.* 39:2673–2689, 2006] and in muscle flaps of residual limbs in patients who underwent transtibial amputation (Portnoy, S., G. Yarnitzky, Z. Yizhar, A. Kristal, U. Oppenheim, I. Siev-Ner, and A. Gefen. *Ann. Biomed. Eng.* 35:120–135, 2007). The goal of the present study was to adapt the method to study the time-dependent mechanical stresses in glutei of patients with SCI during wheelchair sitting, continuously in real-time, and to compare the trends of internal tissue load data with those of controls. Prior to human studies, the real-time FE model—adapted to study the buttocks during sitting—was validated by comparing its predictions to data from a physical phantom of a buttocks and to non-real-time, commercial FE software. Next, real-time, subject-specific, FE models were built for six participating subjects (3 patients with SCI, 3 controls) based on their individual anatomies from MRI scans. Subjects were asked to sit normally in a wheelchair, on a ROHO cushion, and to watch a 90 min movie. Continuous interface pressure measurements from a pressure mat were used as subject-specific boundary conditions for real-time FE analyses of deep muscle stresses. Highest peaks of compression, shear and von Mises stresses throughout the trial period, and averages of peaks of these stresses were recorded over the trial for each individual. These parameters generally had 3-times to 5-times greater values in patients with SCI compared with controls. Likewise, stress doses, defined as the integration of peak compression stress over time, were ~35-times and ~50-times greater in the subjects with SCI, the values referring to the

highest of all peaks recorded throughout the trial, and to average of peaks over the trial, respectively. We believe that by allowing—for the first time—practical and continuous monitoring of internal tissue loads in patients with motosensory deficits, without any risk or interruption to their lifestyle, and either at the clinical setting or at home, the present method can make a substantial contribution to the prevention of severe pressure ulcers and DTI.

**Keywords**—Deep tissue injury, Pressure sore, Decubitus, Paraplegia, Biomechanical model.

## INTRODUCTION

Individuals with a spinal cord injury (SCI) are susceptible to deep tissue injury (DTI), which is a necrosis that onsets in excessively deformed muscle tissue under bony prominences.<sup>5–7</sup> The initial muscle injury may exacerbate to widespread necrosis that extends to fat and skin, and may also lead to osteomyelitis, sepsis, or failure of organ systems.<sup>1,9,14,21,27,42,43</sup> Unfortunately, early detection of DTI is limited by the fact that tissue damage initiates and progresses in deep tissues under intact skin.<sup>37</sup> When the injury becomes visible, usually as a purple or black spot on the skin,<sup>35</sup> damage is already substantial and irreversible, and may require surgical interventions and aggressive medications to be stopped.<sup>23</sup>

In individuals with paraplegia or quadriplegia who use a wheelchair, the gluteus maximus muscles under the ischial tuberosities (ITs) are the most susceptible areas for occurrence and recurrence of serious pressure ulcers and DTI.<sup>46</sup> During sitting, the gluteus maximus muscles are directly overlying the ITs (Figs. 1a and 1b) and are therefore subjected to localized mechanical compression, shear and tension deformations around the highly curved radii of these bony prominences.<sup>25,26</sup> In patients with SCI, significantly higher strains and

Address correspondence to Amit Gefen, Department of Biomedical Engineering, Faculty of Engineering, Tel Aviv University, Tel Aviv 69978, Israel. Electronic mail: gefen@eng.tau.ac.il

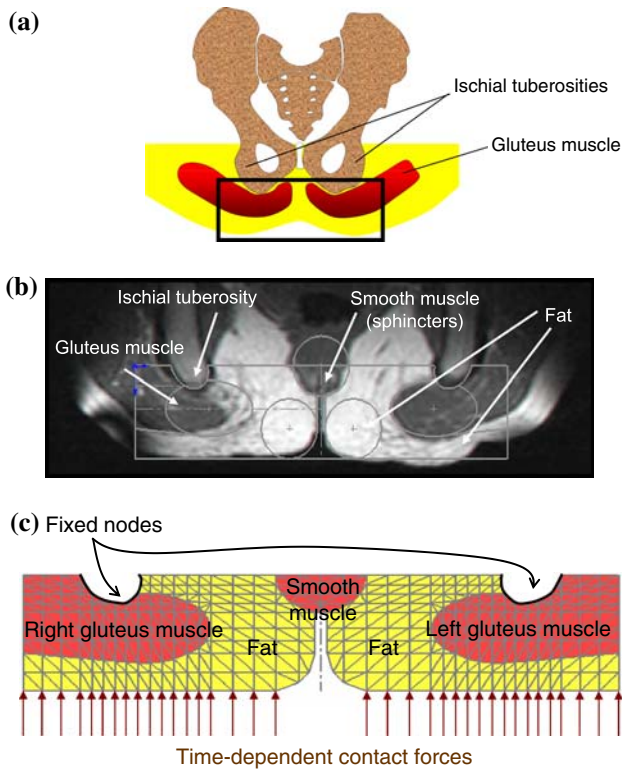


**FIGURE 1.** The real-time finite element (FE) model: (a) the anatomical region of interest in the seated buttocks, showing the glutei muscles under the ischial tuberosities of the pelvis, (b) one example for a coronal MRI scan of a non-weight-bearing buttocks in a sitting-like posture, and (c) the corresponding real-time FE model geometry and mesh for this anatomy.

stresses are formed in the glutei around the ITs compared with controls, as shown in our recent study which integrated MRI scans with patient-specific finite element (FE) models.<sup>26</sup> As the localized tissue loads in the patients with SCI are not relieved through motion, they combine with ischemia, blockage of lymphatic vessels and hindered diffusion to eventually induce and promote muscle cell death.<sup>13,15,18</sup>

In order to understand the etiology of DTI, and perhaps in order to prevent it, strains and stresses in sub-dermal soft tissues overlying bony prominences must be evaluated in individuals continuously in time, in a non-invasive, non-intrusive manner. This means that the internal tissue strains/stresses should be characterized during daily activities, at the patient's natural environment (e.g. home, nursing home, etc.), as opposed to a single laboratory measurement that captures one moment in time. Finite element modeling is a well-established method for biomechanical analyses of soft tissue structures, and indeed, it has been widely used for stress-strain studies of the buttocks.<sup>16,23,30,34,44</sup> Recently, there were studies by our group, as well as by others, employing the FE method in patient-specific models of the buttocks.<sup>25,26,45</sup>

However, all published papers employed the FE models of the buttocks—either “representative” or patient-specific—as a tool for basic research, whereas a more practical, clinically oriented approach for modeling the buttocks of individuals, in order to monitor their internal tissue loads for preventing pressure ulcers in their individual circumstances, is missing in the literature.

Accordingly, the literature summarized above indicates a need for patient-specific FE simulations of internal tissue loads that can be carried out continuously in time, desirably in real-time, and be sensitive to the anatomy and momentary posture of the patient, as well as to the cushioning of his/her wheelchair. Such technology would then allow alerting on over-exposure to internal tissue loads in a clinical setting, at a nursing home or at home, by miniaturization into a portable monitor device.

Recently, we developed a generic real-time, subject-specific FE modeling method to provide monitoring of mechanical conditions in deep tissues deformed between bony prominences and external surfaces. This real-time FE modeling method was previously used by our group in two human studies: Yarnitzky *et al.*<sup>47</sup> first demonstrated feasibility in a setup designed to monitor internal plantar tissue strains and stresses in the foot during treadmill walking. This work was followed by a clinical study of Portnoy *et al.*<sup>33</sup> who adapted the real-time FE system to determine internal strains and stresses in the residual limbs of patients who underwent trans-tibial amputation, again during treadmill walking.

The goals of the present study were to: (i) Adapt the real-time FE method to determine internal tissue loads in the buttocks, in a manner that allows visualization and analysis of gluteal muscle stresses during wheelchair sitting continuously, while considering the individual anatomy, postural changes and cushioning materials. (ii) Conduct human studies with the new experimental system to monitor internal tissue loads in subjects with SCI and in controls during wheelchair sitting, in order to demonstrate the utility of the system and provide the first time-dependent internal tissue stress data for the buttocks' musculature during prolonged sitting. Hence, we provide herein, for the first time, stress-time data for gluteal muscles in a small group of patients with SCI, which overall indicated that their time-dependent gluteal stress state is substantially distinct from that in control subjects.

## METHODS

A simplified subject-specific FE model of a slice through the buttocks was solved in real-time,

continuously, for a time-dependent input of measured interface sitting pressures, using an in-house developed FE code and experimental system. Specifically, the code is able to display time-dependent tissue deformations and calculate the distribution of internal tissue stresses in real-time, by continuously acquiring time-dependant force boundary conditions (BC) from a mat of pressure sensors located between the buttocks of a seated subject and the sitting surface. The model was first verified by comparing real-time predictions of internal tissue stresses in a static condition (i.e. no body movement) with those calculated by a standard commercial, non-real-time FE software (NASTRAN, 2005). The model was then validated against tissue stress measurements conducted using our previous MRI-FE method<sup>25,26</sup> that was considered a gold-standard here, and also, against a specially designed physical phantom of the buttocks. Following the successful validation, human studies were carried out to demonstrate the utility of the real-time FE system. Three patients with SCI and 3 control subjects were monitored with the real-time FE system for 90 min during wheelchair sitting, in order to determine time-dependent deep tissue stresses and stress doses, the latter being defined as stress integrals over time.<sup>11,47</sup> Details on each of these research steps are provided below.

#### *Real-Time Subject-Specific Finite Element Modeling of the Buttocks*

The real-time FE analyses were conducted using a symmetrical, three-dimensional coronal slice through the buttocks, at the location of the ITs (Fig. 1). The model comprised of ITs and enveloping soft tissue structures, including skeletal muscle, smooth muscle, and fat/skin (Figs. 1b and 1c). Fat and skin were considered together, as one effective material (Figs. 1b and 1c). The geometry of the model was defined as parametric, and so, the geometry, and later, the meshing, could be adapted to the individual MRI anatomy (Fig. 1b) in a quick semi-automatic process, by adjusting variables such as the distance between the ITs, the radii of curvature of the ITs, and the mean thicknesses of the glutei and fat/skin layers (Fig. 1c). The thickness of the real-time FE model in the out-of-plane direction was set as 4 mm, corresponding with the slice thickness in the MRI scans used to acquire the anatomy of the buttocks of each individual participant; the protocol of MRI scanning is provided elsewhere.<sup>25</sup>

The model was meshed with between 354 and 420 triangular elements (depending on the subject's anatomy), and meshes contained 594–728 nodes in total (Fig. 1c). To allow real-time continuous stress calculations, muscle and fat/skin tissues were assumed to be

linear elastic materials with elastic moduli of 8.5<sup>31</sup> and 31.9<sup>10</sup> kPa, respectively. Poisson's ratios for these tissues were taken as 0.49.<sup>23</sup> The ITs were considered rigid and all interfaces between adjacent tissue structures (i.e. bone-muscle and muscle-fat/skin) were assigned "no-slip" contact conditions. The distributions of sitting interface pressures, sampled at 1 Hz using a commercial pressure mat (Tactilus, Sensor Products Co., NJ, USA), were continuously fed into the model's code, after conversion to time-dependent BC of force distributions. Specifically, pressure readings from the mat were continuously converted to discrete forces on external ("skin") nodes of the real-time FE mesh facing the pressure mat, by multiplying each pressure reading by the area of the relevant element subjected to the pressure (Fig. 1c). Widths of these superficial elements ranged between 5 and 10 mm (Fig. 1c), and all elements had the same depth, that is, 4 mm which is the thickness of the model.

The hardware composing the experimental system included the pressure mat described above, a connection box with A/D converters, and a PC laptop (2 GHz Pentium 4 processor) to run the real-time FE code (C++, Visual Studio 6.0, Microsoft Co., WA, USA). The theory implemented in the real-time FE code was described by our group in detail in the previous publications of Yarnitzky *et al.*<sup>47</sup> and Portnoy *et al.*,<sup>33</sup> and its sensitivity, numerical accuracy, benefits and drawbacks are described there. For completeness, we provide a short description of the essential components of the real-time FE analysis below.

The real-time FE code continuously solves the linear FE tensorial equation,

$$\mathbf{Kd} = \mathbf{f} \quad (1)$$

where  $\mathbf{K}$  is the stiffness tensor for soft tissues,  $\mathbf{d}$  is the vector of nodal displacements and  $\mathbf{f}$  is the vector of real-time measured interface forces. This equation solves  $n$  number of unknowns, which corresponds to the number of nodal points in the FE mesh. Only the BC force vector  $\mathbf{f}$  (which is measured in real-time) changes between subsequent time steps. The FE set of equations is therefore solved using *LU* decomposition, which provides the optimal time for solution in a case where only the vector of BC is changing between multiple FE solutions. The *LU* decomposition is the product of lower (*L*) and upper (*U*) diagonal matrices that are computed to avoid inverse matrix calculations, which slow down the real-time algorithm.<sup>3,47</sup> The time-complexity for constructing the *LU* matrix is  $O(n^3)$ , but this process is only performed once, at the initiation of the code. The time-complexity for solving the real-time FE problem continuously once the *LU* matrix was calculated is  $O(n^2)$ .<sup>47</sup>

After solving the mesh displacement vector  $\mathbf{d}$ , time-dependent element strains  $e_{kl}(t)$  are calculated, and time-dependent stresses  $s_{ij}(t)$  in the mesh are obtained from the constitutive law,

$$s_{ij}(t) = \mathbf{C}_{ijkl}e_{kl}(t) \quad (2)$$

where  $\mathbf{C}_{ijkl}$  is the isotropic linear elastic constitutive tensor.<sup>33,47</sup>

In order to verify our real-time FE code for numerical accuracy, specifically for the buttocks meshes studied herein, we compared real-time FE calculations for one mesh (of a non-disabled participant)—solved for a static force BC vector, with those of commercial linear FE software (NASTRAN, 2005) for the same mesh and BC, considering same tissue mechanical properties and a linear FE analysis. We found stress differences between the two solvers that were smaller than 5%, across the entire mesh.

#### *Validation of the Real-Time FE Buttocks Models*

The subject-specific real-time FE results were validated by comparing strains calculated in this method to muscle strains obtained from independent processing of MRI images of the same subjects, in a previous study.<sup>26</sup> Additional validation, of stress measures, was achieved by comparing the present real-time FE stresses to experimental muscle stress measurements obtained from a physical phantom of the buttocks. Details on these two validation procedures follow.

#### *Validation Against the MRI-FE Method*

The subject-specific MRI-FE method of analyzing internal tissue strains/stresses in the buttocks was reported elsewhere.<sup>25,26</sup> To describe in brief, weight-bearing and non-weight-bearing MRI scans were obtained from each sitting subject. Subsequently, corresponding individual cross-sectional FE models of the buttocks were developed using a non-linear analysis in MARC software (2005), based on the tissue geometry from the non-weight-bearing MR images. Using a “reverse engineering” approach we then fitted predicted deformed muscle contours (obtained from FE) to measured deformed muscle contours (obtained from MRI), separately for each subject. Then, intramuscular strains were calculated by means of the non-linear large deformation FE models in MARC.<sup>25,26</sup> Principal compression strains along vertical and horizontal paths in the transverse plane of muscles were compared in the present study between the previous MRI-FE method and the currently reported real-time FE model for the same subjects ( $N = 3$ , control subjects only). For each path, the cross-correlation between the previous MRI-FE strain distribution and the present

real-time FE strain distribution was calculated. We also calculated the mean and standard deviation (SD) of errors for each path, in each subject, referring to the previously published MRI-FE data<sup>26</sup> as the gold-standard method.

#### *Validation Against a Physical Phantom of the Buttocks*

A physical phantom of buttocks was built (Fig. 2) according to an MRI scan of the buttocks of a seated female (age: 29 years, bodyweight: 54 kg). The phantom contained a pelvic “bone” made of rigid plastic (elastic modulus 14 MPa, Poisson’s ratio 0.3, Fig. 2a), and enveloping “soft tissues” made of silicone (elastic modulus 1.6 MPa, Poisson’s ratio 0.49, Fig. 2b). Six ultra-thin flexible pressure sensors (FlexiForce, Tekscan Co., MA, USA) were embedded in the phantom, under the ITs, to measure internal pressures in the “soft tissue” substitute, while the phantom is subjected to external loading (Fig. 2a). The external loading was delivered by means of weights, arranged on two rigid vertical metal bars that were connected to the superior aspect of the “pelvis” component of the phantom, above the two artificial ITs (Fig. 2c). A pressure mat (Tactilus, Seonsor Product Co.) was located between the phantom and wheelchair to measure interface (“sitting”) pressures under the projections of the ITs of the phantom. The buttocks phantom was then loaded with the weights, which simulated bodyweights of 50–90 kg at 5 kg-intervals. The weights were mounted on the phantom symmetrically above the two ITs (Fig. 2c), or asymmetrically, such that right or left 15° “pelvic” tilts were produced. The wheelchair’s backrest was first kept erect (90°), and then experiments were repeated for a non-erect (60°) backrest position. These combinations of weight loads and backrest inclinations defined 30 trials in total. For each trial, internal pressure readings under the ITs of the phantom and the corresponding interface “sitting” pressures were recorded simultaneously. Next, the recorded interface pressures were converted to a BC of distributed forces on the external inferior nodes of our real-time FE mesh (as described previously, Fig. 1c), after defining the real-time mesh to represent the specific coronal cross-sectional geometry of the phantom. The mechanical properties of the “bone” and “soft tissue” components of the phantom were fed into the real-time FE model as well. The internal compression stresses under the ITs were then calculated by means of the real-time FE code, for each phantom-simulated static posture (Fig. 2c), to reproduce the phantom experiments computationally. Finally, the measured internal pressure data (phantom) and the calculated internal compression stress data (real-time FE) were

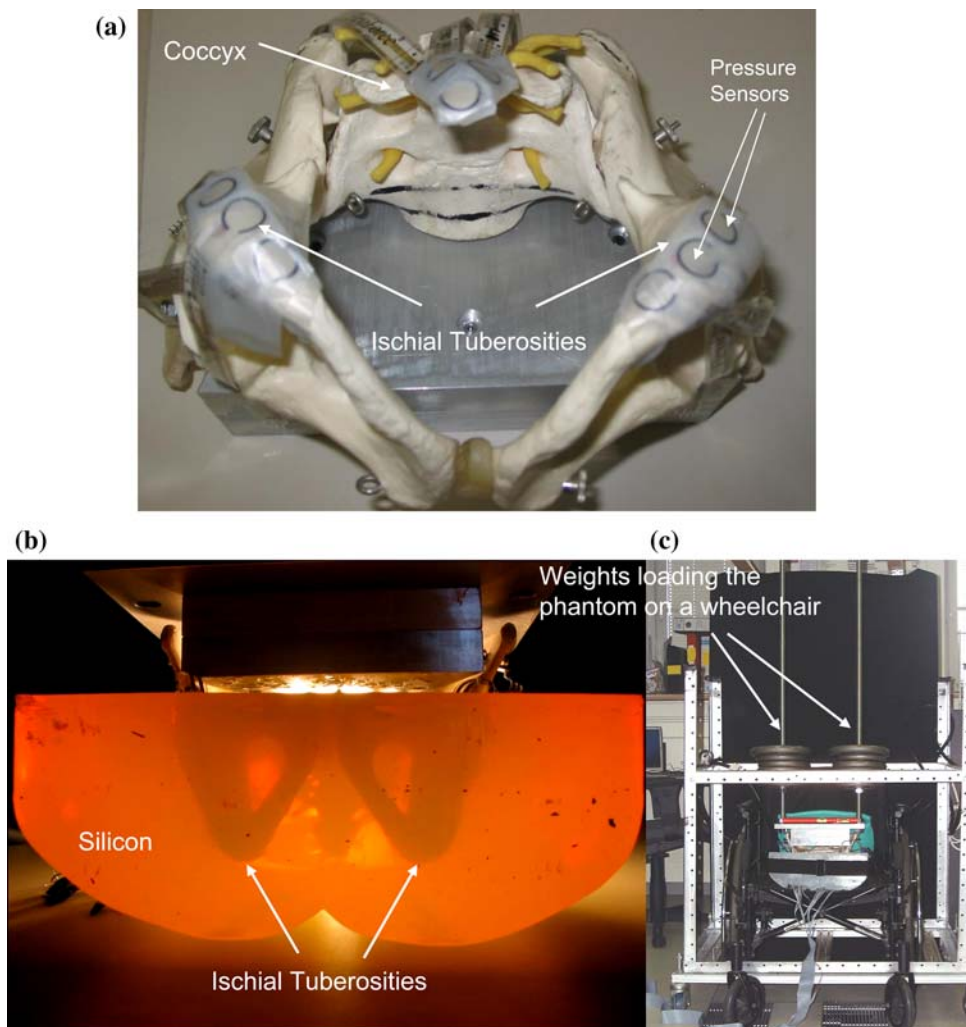


**FIGURE 2.** The physical phantom of the buttocks developed for validation of the real-time finite element (FE) models. (a) Plastic replica of the pelvic bone with pressure sensors adhered to the ischial tuberosities and coccyx. (b) Frontal view of the phantom after molding the silicone structure that represented soft tissues, around the pelvic bone replica. The phantom is illuminated with a high-power light source to visualize the location of the pelvic bone in the silicone cast. (c) The phantom loaded with weights on a wheelchair, in the experimental configuration used to validate the internal stress calculations of the real-time FE system.

compared for each loading case, by means of a Pearson correlation test, and an average-difference (Bland & Altman) plot.<sup>8</sup>

#### *Human Studies*

Six volunteers participated in the studies, of which 3 had no known neuromuscular or orthopedic problems, and so, these were considered controls, and the other 3 depended on a wheelchair for the last 1–17 years, due to a SCI that caused paraplegia (Table 1). Exclusion criteria for the group of patients with SCI were active pressure ulcers and pregnancy. Additionally, we only recruited subjects with SCI who could lift themselves off their wheelchair using their arms, i.e. they were able to completely relieve loads from their buttock's tissues

via push-up maneuvers.<sup>28</sup> These human studies were approved by the Helsinki committee of Sheba Medical Center, Ramat-Gan, Israel (approval #4045/2006), and informed consent was obtained from each participant.

A real-time, subject-specific FE model of a slice through the buttocks at the region of the ITs was built separately for each subject, based on an MRI scan of his/her buttocks during sitting as mentioned earlier in this paper (Fig. 1b), and according to the protocol provided in a previous publication.<sup>25</sup> After defining the geometry of the model, based on the MRI data of the individual (example in Figs. 1b and 1c), the subject was asked to sit normally in a wheelchair, on a commercial wheelchair seat cushion (ROHO, IL, USA), and to watch a movie of his/her choice for 90 min. Subjects with SCI used their own wheelchairs, whereas controls

**TABLE 1. Body characteristics of subjects and relevant medical information for the patient group.**

Parameter	Controls			Subjects with spinal cord injury		
	EG	SP	ID	YB <sup>a</sup>	RW	HZ
Gender	Male	Female	Male	Male	Female	Male
Bodyweight (kg)	85	55	78	80	70	90
Age (years)	28	29	27	43	36	21
Level of spinal injury <sup>b</sup>	N/A			T12	T3	T6
Years post-spinal injury	N/A			9	17	1
Horizontal distance between IT <sup>c</sup> (mm)	120	142	108	122	140	123
Right IT radius of curvature <sup>c</sup> (mm)	12	13	11	13	24	21
Left IT radius of curvature <sup>c</sup> (mm)	10	10	13	12	20	21
Gluteus thickness under the right IT <sup>c</sup> (mm)	20	27	20	29	8	3
Gluteus thickness under the left IT <sup>c</sup> (mm)	26	21	19	28	5	6
Fat thickness under the right IT <sup>c</sup> (mm)	21	13	10	11	8	15
Fat thickness under the left IT <sup>c</sup> (mm)	16	14	12	12	7	13

N/A not applicable; IT ischial tuberosities.

<sup>a</sup>Subject #1 in the group of subjects with spinal cord injury is involved in professional athletic activity, which can explain the greater thickness of his gluteal muscles with respect to others in this group.

<sup>b</sup>Injuries were located at the thoracic (T) spine for all the subjects with spinal cord injury.

<sup>c</sup>Data measured while subjects sat at a non-weight-bearing posture.<sup>25,26</sup>

used a standard manual hospital wheelchair. Continuous interface pressure measurements were acquired between the patient's buttocks and the cushion, via the pressure mat. Pressure data were communicated to a PC laptop in real-time, for the real-time FE analysis of deep tissue stresses in the individuals (Fig. 3). The peaks of principal compression stresses, tension stresses, shear stresses and von Mises stresses occurring in the gluteus muscles were recorded for the 90 min sitting trials, from the raw internal stress distributions at each timeframe (1 frame per second, Figs. 3 and 4). The highest peak stress occurring throughout the 90 min trial was registered for each of the above stress components, and additionally, the means of peak stress values recorded at each second over the 90 min period were calculated. Stress doses in the gluteus muscles were also calculated, by numerically integrating the peak compression stress in muscle tissue over time, at time steps of 1 s, between two consecutive internal tissue load relief events (Fig. 4c). An internal tissue load relief event was defined to occur when the peak compression stress value in the gluteus was below 2 kPa for at least 1 s. The 2 kPa threshold was selected to indicate relief based on our previous animal studies, where muscle tissue was found to be able to tolerate compression stresses of 2 kPa without loss of viability for 6 h.<sup>22</sup> Analogically to the processing of stress data, a peak stress dose for the entire 90-min trial was registered, and a mean of the stress doses recorded between consecutive internal tissue load relief events was calculated over the 90 min period. Finally, the number of internal tissue load relieves during 90 min of sitting was calculated by counting the number of

below-2 kPa peak muscle stress readings that lasted at least 1 s over the 90 min trial period (Fig. 4c). All stress and stress dose outcome measures were calculated separately, and simultaneously, for the left and right sides of the body.

## RESULTS

### *Validation Studies*

Examples of strain distributions calculated using the previous, gold-standard MRI-FE method<sup>25,26</sup> (solid line), and also, using the present real-time subject-specific FE method (dashed line), are shown in Fig. 5 for one control subject, named "ID" in Table 1 (male, age 27 years, bodyweight 78 kg). Specifically, the comparison between the MRI-FE and real-time FE strain distribution data are made along path *N*, crossing the gluteus muscle vertically under the ITs, and along path *M*, which follows the centerline of the muscle, for the right gluteus muscle, and for an upright sitting posture (see also the path definitions in the top frame of Fig. 5). It is evident that the two curves—from the two methods—are very similar for each path (Figs. 5a and 5b). Indeed, a quantitative analysis indicated that cross-correlations between strain distribution curves along the muscle contours *N*, *M*—calculated from MRI-FE and using real-time FE—did not drop below 0.8, for all 6 subjects. Moreover, the mean error between the strain curves from the two methods was smaller than 10% strain, and the SD of the error was kept below 5% strain, for each subject.

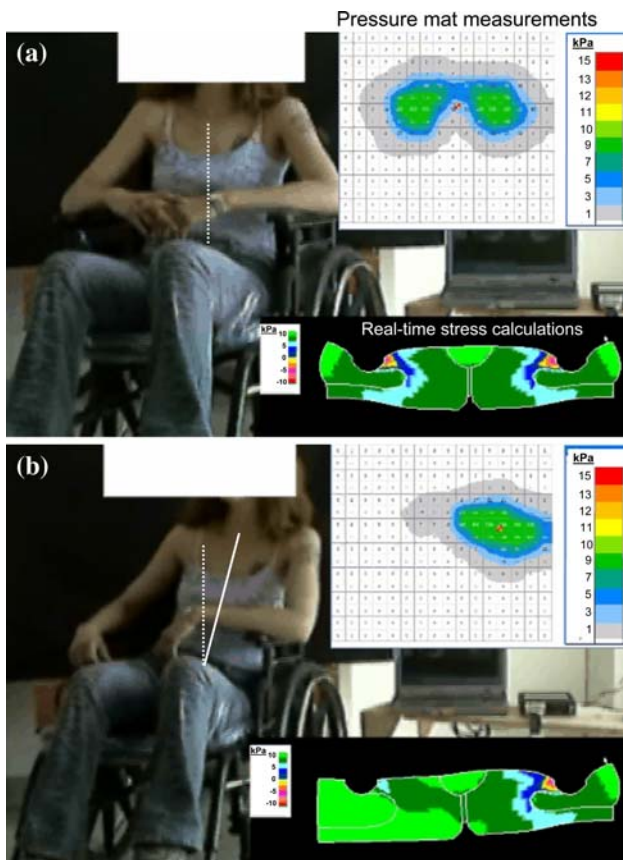


**FIGURE 3.** Examples of the real-time finite element (FE) model inputs of pressure mat measurements (top right frames), and corresponding outputs of real-time internal tissue stress distributions (bottom right frames) for two momentary postures of a control subject from one trial: (a) balanced erect sitting and (b) a tilt of the trunk to the left. The real-time FE model responses, of similar left/right tissue deformations and internal stresses for the left/right body sides in posture (a), as opposed to a marked unilateral deformation of the left gluteus for posture (b), are clearly shown.

Likewise, the internal compression stresses calculated using the real-time FE system were in very good agreement with internal pressures measured by the sensors embedded in the physical phantom of the buttocks (Fig. 6). Specifically, the squared Pearson correlation coefficient when regressing between the real-time FE stress data and the corresponding experimental internal pressure readings under the ITs exceeded 0.98 (Fig. 6a). The mean value of the predictive error of the real-time FE model with respect to the measurements from the buttocks phantom was found to be  $4 \pm 4$  kPa (for 30 experiments carried out with different loads and postures, as described in “Methods” section). The average-difference plot indicated that all maximal peak stress data points were well within the  $\pm 2SD$  lines of agreement (Fig. 6b). It is further indicated by these comparisons, and particularly by the plot in Fig. 6a, that the real-time FE

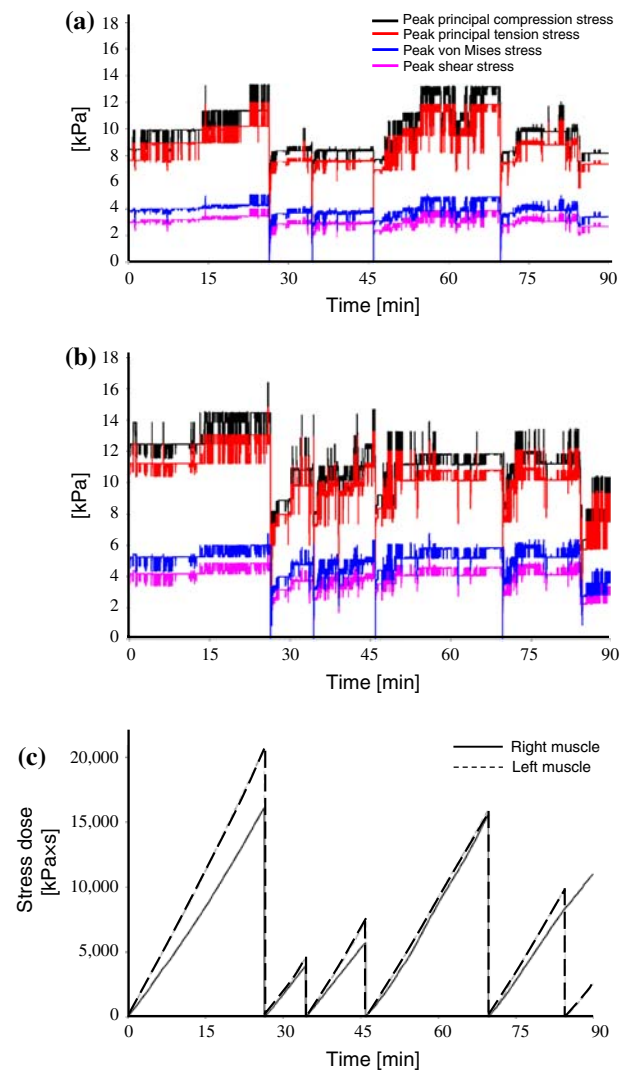


**FIGURE 4.** Examples of raw stress data from the real-time finite element analysis for one patient with spinal cord injury over the entire 90 min sitting session. The plots specifically show peak principal compression, principal tension, von Mises and shear stresses calculated in the right (a) and left (b) gluteus muscles, as well as peak stress doses calculated at the two body sides (c).

system tended to mildly overestimate the internal pressure readings from the phantom for low internal compression stresses (that is, below 30 kPa), and also, that the real-time FE tended to mildly underestimate the pressure readings for the high internal compression stress domain (i.e. more than 60 kPa) (Fig. 6a). Around the midrange of internal tissue loads (compression stresses of 30–60 kPa), the agreement between real-time FE and phantom measurements was at best (Fig. 6a), and so, differences were mostly within  $\pm 1SD$  lines of agreement (Fig. 6b). We noticed these trends in data for all the simulated postures (that is, erect or non-erect, pelvis tilting to the side or not).

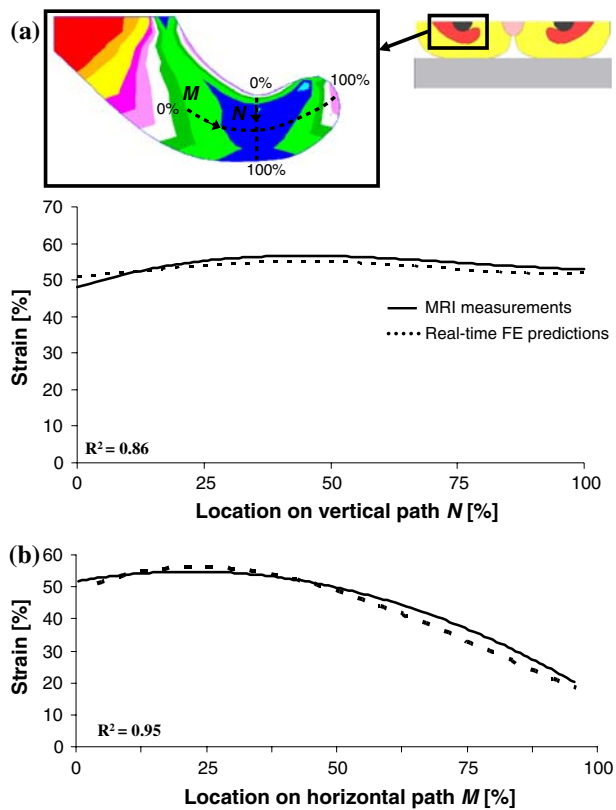


**FIGURE 5.** Validation of the real-time finite element (FE) strain data against corresponding gold-standard MRI-FE results, for the same control subject (male, age 27 years, bodyweight 78 kg, named “ID” in Table 1). The data describe muscle strains during upright static sitting in a wheelchair. The distributions of strains along path *N* (a), and along path *M* (b), as defined in the top frame, are shown in solid lines for MRI-FE data and in dashed lines for the real-time FE data.

### Human Studies

Using the real-time FE method and experimental system, we were able to monitor internal tissue stress data for continuous 90 min of sitting, at the daily environment of subjects, that is, patients with SCI were studied at their homes and control subjects were studied at our Musculoskeletal Biomechanics Laboratory, where they are employed. In all trials, the muscle stress distribution data were displayed online (but not shown to the subjects during the trial), and also, stress data were saved to files for post-processing. We therefore demonstrated that the technology is feasible, and is ready to use in larger-scale clinical trials either with or without feedback to the patient.

Outcome measures of stresses and stress doses were generally substantially greater in the subjects with SCI, with respect to controls (Figs. 7–9). Specifically, the highest of all peak gluteal stress values which occurred throughout the 90 min trials, and the average of peak gluteal stresses over the 90 min sitting sessions, were

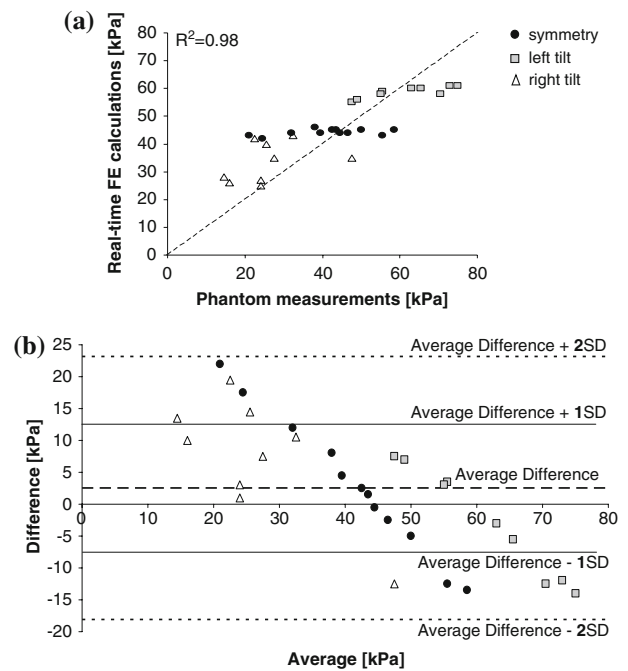


**FIGURE 6.** Validation of the real-time finite element (FE) stress data against measurements from the buttocks phantom system (shown in Fig. 2). (a) Principal compression stresses calculated by the real-time FE system adapted for the buttocks phantom, plotted vs. the internal pressure readings under the artificial ischial tuberosities of the phantom, as recorded by the sensors in the buttocks phantom system. The individual trials simulated different postures, including 15° pelvis tilts and leaning backward (backrest at 60°). The unity line, indicating a theoretical perfect agreement between the two measurement systems, is depicted as a dashed line. (b) Average-difference (Bland & Altman) plot<sup>8</sup> depicting the agreement between compression stresses calculated using real-time FE, and internal pressure readings from the buttocks phantom.

3-times to 5-times greater in the subjects with SCI compared with the controls (Figs. 7 and 8). Consistent with the peak stress magnitudes during sitting, the highest of, and the average of all peak stress dose values in the gluteus muscles were ~35-times and ~50-times greater in subjects with SCI compared with the controls (Figs. 9a and 9b). Using our criterion of peak muscle compression stress below 2 kPa for at least 1 s as an indicator of an internal tissue load relief event, the number of relieves during the 90 min trials was ~10-times greater in controls with respect to the individuals with SCI (Fig. 9c).

### DISCUSSION

In this study, we focused—from a basic science aspect—on stress-time exposures in glutei during sitting for patients with paraplegia and normals, and, on the application side, we presented a technology for



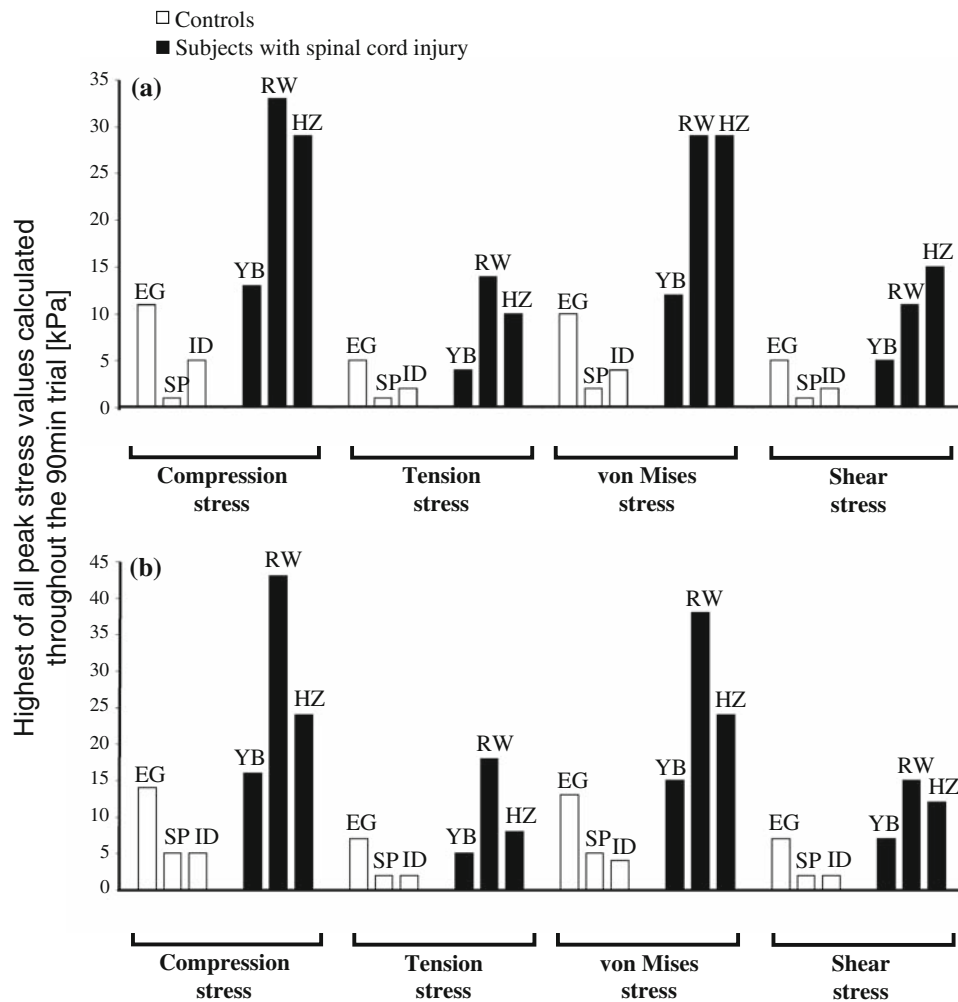


**FIGURE 7.** Highest of all peak stress values occurring throughout the 90 min trials in the gluteus muscles of subjects with spinal cord injury and controls, for the (a) right and (b) left glutei of each individual participant. The sampling frequency was 1 Hz. Note that stress scales differ between the left and right body sides.

potentially alerting on conditions that may lead to DTI. The traditional and most commonly accepted medical indicator for evaluating a risk for pressure ulcers was for 30 years or so, and still is, interface pressures.<sup>12,40</sup> A review of the literature specifically shows that monitoring interface pressures over time for preventing pressure ulcers had been around from as early as the late 1970s, when Temes and Harder<sup>41</sup> designed a system which activates an alarm when sensors did not detect a relief of interface pressures. Likewise, shortly after this publication, Patterson and Fisher<sup>32</sup> measured interface pressures under the ischia of paraplegic subjects during wheelchair sitting, and counted pressure relieves. Merbitz *et al.*<sup>28</sup> built a monitoring system on the 1980's which measured time intervals between interface pressure relieves during wheelchair sitting for long-term periods, and more recently, in this millennium, Stockton and Parker<sup>39</sup>

conducted a large-scale survey of interface pressure relief behaviors among more than a hundred wheelchair users. The patent literature is similarly rich in inventions that are based on the application of interface pressure measurements for the prevention of pressure ulcers, e.g. US Patent 6030351 "Pressure relief reminder and compliance system", 2000, or US Patent 6287253 "Pressure ulcer condition sensing and monitoring", 2001. Albeit this vast and thorough research work, that lasts for more than 3 decades, the problem of pressure ulcers and DTI is far from a resolution, which is a rather strong indication that interface pressures are not the right parameter to look at.<sup>17</sup>

Indeed, and as already explained in the Introduction, more recent studies define the pathogenesis of serious pressure ulcers, or DTI, as a deep tissue damage preceding skin damage<sup>4,5,7,29</sup> whereas the initial damage is caused mostly by the sustained internal

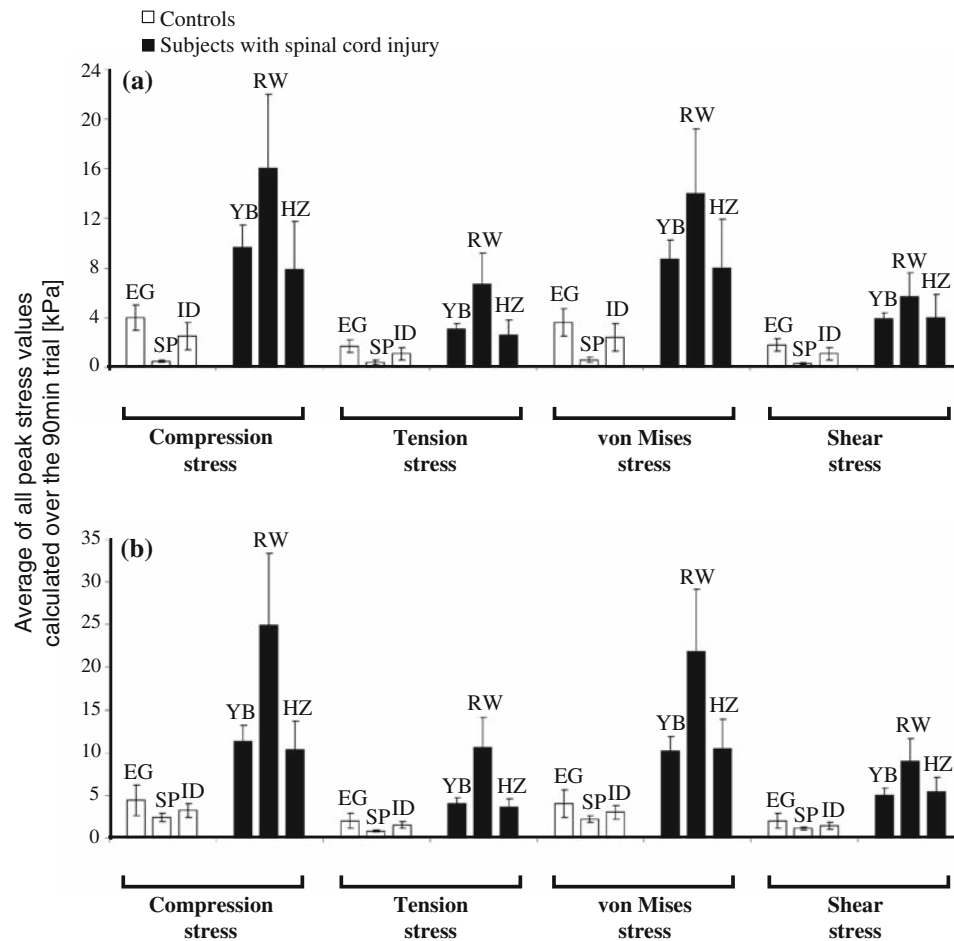


**FIGURE 8.** Average of all peak stress values calculated over the 90 min trials in the gluteus muscles of subjects with spinal cord injury and controls, for the (a) right and (b) left glutei of each individual participant. Error bars indicate intra-subject standard deviation of data. The sampling frequency was 1 Hz. Note that stress scales differ between the left and right body sides.

strains and stresses in internal soft tissues deformed under bony prominences.<sup>37,38</sup> These deep tissue strains/stresses cannot be quantified by means of interface pressure measurements *per se*, and require more sophisticated methods, that is, biomechanical models of the buttocks anatomy that also consider how strains and stresses are distributed in the internal tissue structures, depending on geometrical and mechanical property factors.<sup>17,23,25,26,30</sup> Here, we propose—for the first time—a method and system to monitor deep tissue loads and load distributions in the buttocks of individuals continuously and in real-time, based on the FE numerical technique. Moreover, we apply this new real-time FE analysis of the seated buttocks to explore trends of differences between internal load parameters of patients with SCI and controls.

We found substantially higher stresses in muscles under the ITs of patients with SCI with respect to controls (Fig. 7), which indicates that the present

method and system could clearly identify that the paraplegic patients are more susceptible to pressure ulcers and DTI. This nicely agrees with our previous findings from MRI-FE studies,<sup>25,26</sup> which were considered here as the gold-standard method of determining internal tissue strains/stresses in the load-bearing buttocks. These previous MRI-FE studies revealed that biomechanical conditions in muscle tissue are highly influenced by the anatomical changes associated with paraplegia—mainly loss of gluteal muscle thickness and shape changes of the ITs—that lead to localized elevated strains and stresses in muscle tissue under the ITs (Table 1). The strength of the present real-time FE method and system is in its ability to monitor these stress exposures over time depending on the posture (e.g. lateral tilt of the trunk vs. upright sitting), wheelchair design and cushioning material. The present data, though from small subject groups, indicate that postural behaviors, in particular, vary substantially even between control subjects. For

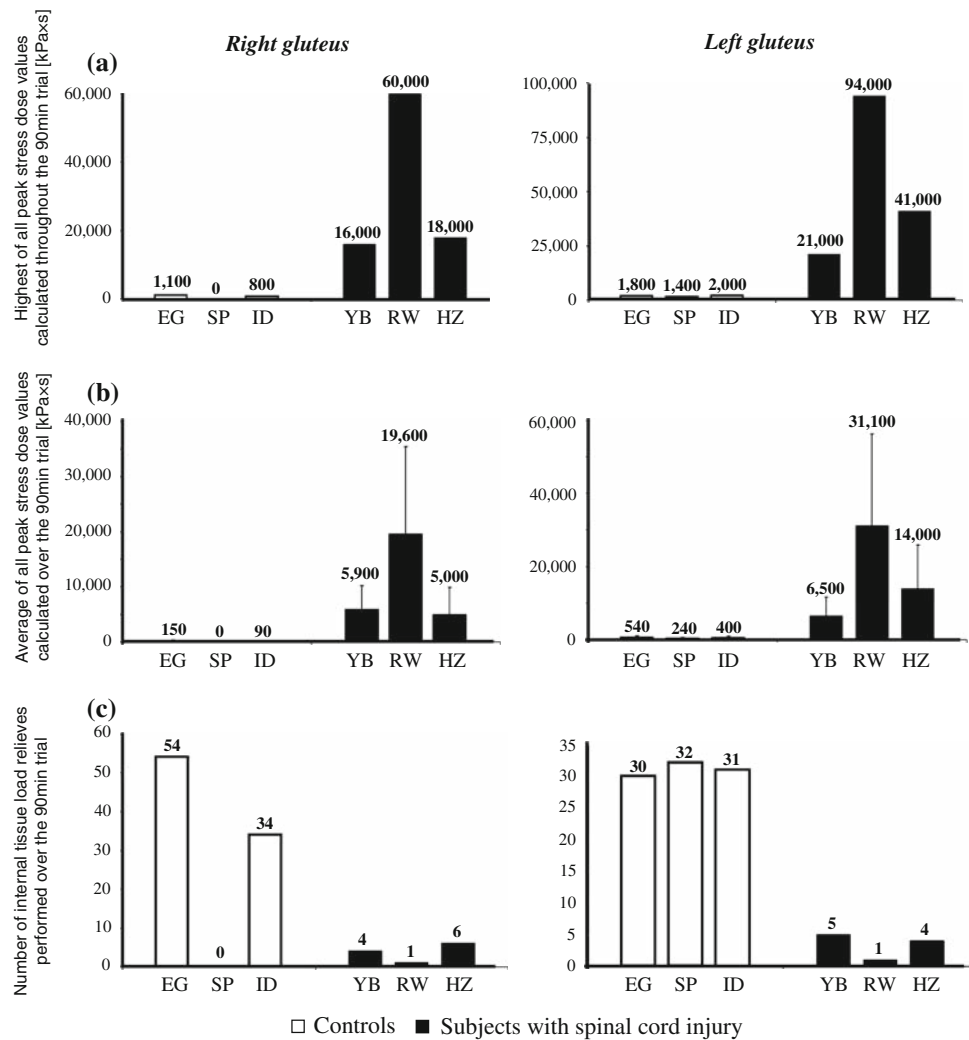


**FIGURE 9.** Compression stress doses and internal tissue load relieves in subjects with spinal cord injury and controls: (a) The highest of all peak stress doses occurring throughout the 90 min trials, (b) the average of all peak stress doses calculated over the 90 min trials, with error bars indicating intra-subject standard deviation, and (c) the number of internal tissue load relieves performed over the 90 min trials, for each individual participant. An internal tissue load relief event was defined to occur when the peak compression stress value in a gluteus muscle was below 2 kPa for at least 1 s. The sampling frequency was 1 Hz. Note that scales differ between parameters of the left and right body sides.

example, control subject SP sat with a tendency to the left body side during the whole trial, and she therefore showed distinctly low (negligible) stress doses and internal tissue load relief values at her right body side, with respect to the other two control subjects (Fig. 9). The observation that sitting behaviors differ substantially across healthy individuals is consistent with our previous studies,<sup>24</sup> which highlighted a variability in time intervals between postural changes of normals during prolonged wheelchair sitting sessions. Moreover, data in Figs. 7–9 indicate that among the subjects with SCI there are higher intra-subject as well as inter-subject variabilities in stress and stress dose parameters, with respect to controls. The SCI therefore adds to an existing level of variability in motor behaviors

during sitting, because internal tissue load relieves post-SCI also depend on the neuromuscular aspects of severity of the SCI as well as on the outcomes of the rehabilitation program, and the motivation of the patient to change postures for preventing pressure ulcers.<sup>19,36,39</sup>

The ability of the present method and system to monitor the consequences of this individual motor behavior on the exposure to internal tissue loads is unique and has numerous applications in rehabilitation and pressure ulcer prevention programs. For example, it can be used for providing feedback to the patient regarding the momentary risk for him/her to develop a DTI while he/she is in the rehabilitation program or at home during daily activities. It can also

be used to monitor the patient's behavior over time, in order to allow him/her to be better aware of their risk at a given time compared with past performances, e.g. in following a routine of push-up maneuvers with their hands<sup>28</sup> to decrease time exposures to sustained internal tissue loads. In this context, it should be mentioned that the numbers of internal tissue load relief events detected by our real-time FE system for the SCI group during the 90 min sessions (Fig. 9c) is in general agreement with previous studies where such relieves were counted over time based on interface pressure measurements.<sup>28,32,39</sup>

An important feature of the real-time FE method and system is that they can be programmed to include a tissue injury threshold which allows continuous evaluation of the likelihood for biological damage (e.g. cell death due to deformation, or due to ischemia, or both). Such tissue injury thresholds recently became available for skeletal muscle, in terms of compression stress or strain as the measure for internal tissue loading,<sup>18,22</sup> and since these injury thresholds have a closed-form mathematical formulation, they can be integrated in a straight-forward manner into the present system.

An additional strength of the present real-time FE method and system is its ability to consider different cushioning materials for the sitting surface of the wheelchair, which allows the rehabilitation practitioners, and the patient him/herself, to visually and quantitatively observe the effect of replacing a cushion on deep tissue stresses and stress exposures. Even changing the inflation pressures of the ROHO cushion influences the deep tissue stresses, by affecting the interface pressures<sup>20</sup> which are being used as input BC to the real-time FE model. Although the issue of cushioning was not directly addressed in the present study, we see a great potential of the real-time FE method and system as an objective and effective, and perhaps someday a standard bioengineering tool to evaluate, rate and eventually select the cushion or the cushion parameters (e.g. the ROHO inflation pressure) that best meet the needs of the individual patient—in terms of lowering internal tissue loads. It should be mentioned that lowering internal tissue loads is not the only consideration in selecting a cushion (others include, for example, comfort and postural support), but it is certainly one of the central considerations. We therefore intend to explore the effects of cushion design, including shape, material parameters and inflation pressures if applicable, in future studies. Similarly important are the adjustments of the wheelchair to the individual, e.g. the height of the footrests and armrests. There might be a tradeoff between maximizing patient functionalities by means of these adjustments and still achieving low levels of internal

tissue loads, but in this regard as well, the present method and system allow objective measurements of tissue loads and immediate feedback.

Trends in the present subject stress data, i.e. that gluteal stress and stress dose values are greater in subjects with SCI with respect to controls (Figs. 7–9), are consistent with the recent Agam and Gefen<sup>2</sup> study who used a comparable experimental design, but employed real-time Hertzian contact analysis with simplified bone/muscle model geometry, rather than real-time FE. The main limitations of the present real-time subject-specific FE modeling are the use of a linear FE theory, and still, a relatively simple geometry—both meant to allow the calculation of stress distribution data in real-time. A complete and detailed discussion regarding the limitations of the real-time FE modeling method can be found in Yarnitzki *et al.*<sup>47</sup> and in Portnoy *et al.*<sup>33</sup> However, in our opinion, the utility of the real-time FE method and system in the clinical setting, as opposed to just basic research, overweigh its limitations, particularly considering the extensive validation work described in this paper which did not, eventually, indicate major differences between real-time FE predictions and off-line non-linear large deformation FE analyses. In regard to the accuracy of real-time FE as indicated by the present validation studies: we found that the real-time FE tended to mildly overestimate compression stresses in the lower stress domain (<30 kPa), and it mildly underestimated stresses in the higher stress domain (>60 kPa), as shown in Fig. 6a. However, our previous MRI-FE (gold-standard) studies<sup>26</sup> demonstrated that physiological internal peak compression stresses in gluteal muscle tissue during sitting range between approximately 30 kPa (for non-disabled subjects) to about 60 kPa (for patients with paraplegia due to SCI). This is exactly the domain where the real-time FE system shows its best accuracy, as manifested by the average-difference plot in Fig. 6b.

In closure, the present real-time FE method and system can be applied in the future to several potential medical applications. For example, it can be used as a part of an alarm system which announces the patient or his/her caretakers about critical internal tissue loads during wheelchair sitting, or while lying in bed. Likewise, it can be used in the process of selection of a wheelchair cushion, or perhaps in the design of wheelchairs and cushions. It can also provide feedback to the insensitive patient on his deep tissue loads as related to his sitting habits, which is useful for rehabilitation and education for pressure ulcer prevention. The utility of the real-time FE method and system can be extended to study not just SCI patients but also other vulnerable populations, e.g. geriatric patients or patients with degenerative neuromuscular diseases.

We believe that the present technology can make a substantial contribution to lowering the prevalence of severe pressure ulcers, thereby minimizing both the suffering caused by these devastating wounds, and their enormous healthcare costs.

### ACKNOWLEDGMENTS

We appreciate the help of Mr. Boaz Samir from “Zeadim” Daily Rehabilitation Center, Ramat-Gan, Israel, for his help in recruiting volunteers for this study. Ms. Sigal Portnoy, a doctoral student in the Musculo-skeletal Biomechanics Laboratory (AG), Tel Aviv University, is thanked for her help in data analyses.

### REFERENCES

- <sup>1</sup>Agam, L., and A. Gefen. Pressure ulcers and deep tissue injury: a bioengineering perspective. *J. Wound Care* 16: 336–342, 2007.
- <sup>2</sup>Agam, L., and A. Gefen. Toward real-time detection of the risk for a deep tissue injury in wheelchair users using the Hertz contact theory. *J. Rehabil. Res. Dev.* 45:537–550, 2008.
- <sup>3</sup>Berkley, J., G. Turkiyyah, D. Berg, M. Ganter, and S. Weghorst. Real-time finite element modeling for surgery simulation: an application to virtual suturing. *IEEE Trans. Vis. Comput. Graph.* 10:314–325, 2004. doi:10.1109/TVCG.2004.1272730.
- <sup>4</sup>Berlowitz, D. R., and D. M. Brienza. Are all pressure ulcers the result of deep tissue injury? A review of the literature *Ostomy Wound Manage.* 53:34–38, 2007.
- <sup>5</sup>Black, J. Deep tissue injury: state of the science. In: 10th European Pressure Ulcer Advisory Panel Open Meeting, Oxford, UK, August 30–September 1, 2007.
- <sup>6</sup>Black, J. M., and The National Pressure Ulcer Advisory Panel. Moving towards consensus on deep tissue injury and pressure ulcer staging. *Adv. Skin Wound Care* 18:415–421, 2005. doi:10.1097/00129334-200510000-00008.
- <sup>7</sup>Black, J., M. Baharestani, J. Cuddigan, B. Dörner, L. Edsberg, D. Langemo, M. E. Posthauer, C. Ratliff, G. Taler, and National Pressure Ulcer Advisory Panel. National Pressure Ulcer Advisory Panel’s updated pressure ulcer staging system. *Dermatol. Nurs.* 19:343–349, 2007.
- <sup>8</sup>Bland, J. M., and D. G. Altman. Statistical methods for assessing agreement between two methods of clinical measurement. *Lancet* i:307–310, 1986.
- <sup>9</sup>Bliss, M. R. Acute pressure area care: Sir James Paget’s legacy. *Lancet* 339:221–223, 1992. doi:10.1016/0140-6736(92)90016-V.
- <sup>10</sup>Brosh, T., and M. Arcan. Modeling the body/chair interaction—an integrative experimental-numerical approach. *Clin. Biomech.* 15:217–219, 2000. doi:10.1016/S0268-0033(99)00073-X.
- <sup>11</sup>Drerup, B., S. Kraneburg, and A. Koller. Visualisation of pressure dose: synopsis of peak pressure, mean pressure, loading time and pressure time-integral. *Clin. Biomech.* 16:833–834, 2001.
- <sup>12</sup>Ferrarin, M., G. Andreoni, and A. Pedotti. Comparative biomechanical evaluation of different wheelchair seat cushions. *J. Rehabil. Res. Dev.* 37:315–324, 2000.
- <sup>13</sup>Gawlitta, D., W. Li, C. W. Oomens, F. P. Baaijens, D. L. Bader, and C. V. Bouten. The relative contributions of compression and hypoxia to development of muscle tissue damage: an *in vitro* study. *Ann. Biomed. Eng.* 35:273–284, 2007. doi:10.1007/s10439-006-9222-5.
- <sup>14</sup>Gefen, A. The biomechanics of sitting-acquired pressure ulcers in patients with spinal cord injury or lesions. *Int. Wound J.* 4:222–231, 2007. doi:10.1111/j.1742-481X.2007.00330.x.
- <sup>15</sup>Gefen, A., L. H. Cornelissen, D. Gawlitta, D. L. Bader, and C. W. Oomens. The free diffusion of macromolecules in tissue-engineered skeletal muscle subjected to large compression strains. *J. Biomech.* 41:845–853, 2008. doi:10.1016/j.jbiomech.2007.10.023.
- <sup>16</sup>Gefen, A., N. Gefen, E. Linder-Ganz, and S. S. Margulies. *In vivo* muscle stiffening under bone compression promotes deep pressure sores. *J. Biomech. Eng.* 127:512–524, 2005. doi:10.1115/1.1894386.
- <sup>17</sup>Gefen, A., and J. Levine. The false premise in measuring body-support interface pressures for preventing serious pressure ulcers. *J. Med. Eng. Tech.* 31:375–380, 2007. doi:10.1080/03091900601165256.
- <sup>18</sup>Gefen, A., B. van Nierop, D. L. Bader, and C. W. Oomens. Strain-time cell-death threshold for skeletal muscle in a tissue-engineered model system for deep tissue injury. *J. Biomech.* 41:2003–2012, 2008. doi:10.1016/j.jbiomech.2008.03.039.
- <sup>19</sup>Giltsdorf, P., R. Patterson, and S. Fisher. Thirty-minute continuous sitting force measurements with different support surfaces in the spinal cord injured and able-bodied. *J. Rehabil. Res. Dev.* 28:33–38, 1991. doi:10.1682/JRRD.1991.10.0033.
- <sup>20</sup>Hamanami, K., A. Tokuhiko, and H. Inoue. Finding the optimal setting of inflated air pressure for a multi-cell air cushion for wheelchair patients with spinal cord injury. *Acta. Med. Okayama* 58:37–44, 2004.
- <sup>21</sup>Levi, B., and R. Rees. Diagnosis and management of pressure ulcers. *Clin. Plast. Surg.* 34:735–748, 2007. doi:10.1016/j.cps.2007.07.007.
- <sup>22</sup>Linder-Ganz, E., S. Engelberg, M. Scheinowitz, and A. Gefen. Pressure-time cell death threshold for albino rat skeletal muscles as related to pressure sore biomechanics. *J. Biomech.* 39:2725–2732, 2006. doi:10.1016/j.jbiomech.2005.08.010.
- <sup>23</sup>Linder-Ganz, E., and A. Gefen. Mechanical compression-induced pressure sores in rat hind-limb: muscle stiffness, histology and computational models. *J. Appl. Physiol.* 96:2034–2049, 2004. doi:10.1152/jappphysiol.00888.2003.
- <sup>24</sup>Linder-Ganz, E., M. Scheinowitz, Z. Yizhar, S. S. Margulies, and A. Gefen. How do normals move during prolonged wheelchair-sitting? *Technol. Health Care* 15:195–202, 2007.
- <sup>25</sup>Linder-Ganz, E., N. Shabshin, Y. Itzchak, and A. Gefen. Assessment of mechanical conditions in sub-dermal tissues during sitting: a combined experimental-MRI and finite element approach. *J. Biomech.* 40:1443–1454, 2007. doi:10.1016/j.jbiomech.2006.06.020.
- <sup>26</sup>Linder-Ganz, E., N. Shabshin, Y. Itzchak, Z. Yizhar, I. Siev-Ner, and A. Gefen. Strains and stresses in sub-dermal tissues of the buttocks are greater in paraplegics than in healthy during sitting. *J. Biomech.* 41:567–580, 2008. doi:10.1016/j.jbiomech.2007.10.011.

- <sup>27</sup>Margolis, D. J., J. Knauss, W. Bilker, and M. Baumgarten. Medical conditions as risk factors for pressure ulcers in an outpatient setting. *Age Ageing* 32:259–264, 2003. doi:[10.1093/ageing/32.3.259](https://doi.org/10.1093/ageing/32.3.259).
- <sup>28</sup>Merbitz, C. T., R. B. King, J. Bleiberg, and J. C. Grip. Wheelchair push-ups: measuring pressure relief frequency. *Arch. Phys. Med. Rehabil.* 66:433–438, 1985.
- <sup>29</sup>Ohura, T., N. Ohura, and H. Oka. Incidence and clinical symptoms of hourglass and sandwich-shaped tissue necrosis in stage IV pressure ulcers. *Wounds* 19:310–319, 2007.
- <sup>30</sup>Oomens, C. W., O. F. Bressers, E. M. Bosboom, C. V. Bouten, and D. L. Bader. Can loaded interface characteristics influence strain distributions in muscle adjacent to bony prominences? *Comput. Met. Biomech. Biomed. Eng.* 6:171–180, 2003. doi:[10.1080/1025584031000121034](https://doi.org/10.1080/1025584031000121034).
- <sup>31</sup>Palevski, A., I. Glaich, S. Portnoy, E. Linder-Ganz, and A. Gefen. Stress relaxation of porcine gluteus muscle subjected to sudden transverse deformation as related to pressure sore modeling. *J. Biomech. Eng.* 128:782–787, 2006. doi:[10.1115/1.2264395](https://doi.org/10.1115/1.2264395).
- <sup>32</sup>Patterson, R. P., and S. V. Fisher. Pressure and temperature patterns under ischial tuberosities. *Bull. Prosthet. Res.* 17:5–11, 1980.
- <sup>33</sup>Portnoy, S., G. Yarnitzky, Z. Yizhar, A. Kristal, U. Oppenheim, I. Siev-Ner, and A. Gefen. Real-time patient-specific finite element analysis of internal stresses in the soft tissues of a residual limb: a new tool for prosthetic fitting. *Ann. Biomed. Eng.* 35:120–135, 2007. doi:[10.1007/s10439-006-9208-3](https://doi.org/10.1007/s10439-006-9208-3).
- <sup>34</sup>Ragan, R., T. W. Kernozek, M. Bidar, and J. W. Matheson. Seat-interface pressures on various thicknesses of foam wheelchair cushions: a finite modeling approach. *Arch. Phys. Med. Rehabil.* 83:872–875, 2002. doi:[10.1053/apmr.2002.32677](https://doi.org/10.1053/apmr.2002.32677).
- <sup>35</sup>Salcido, R. What is the “purple heel”? *Adv. Skin Wound Care* 19:11, 2006.
- <sup>36</sup>Shirado, O., M. Kawase, A. Minami, and T. E. Strax. Quantitative evaluation of long sitting in paraplegic patients with spinal cord injury. *Arch. Phys. Med. Rehabil.* 85:1251–1256, 2004. doi:[10.1016/j.apmr.2003.09.014](https://doi.org/10.1016/j.apmr.2003.09.014).
- <sup>37</sup>Stekelenburg, A., C. W. Oomens, G. J. Strijkers, K. Nicolay, and D. L. Bader. Compression-induced deep tissue injury examined with magnetic resonance imaging and histology. *J. Appl. Physiol.* 100:1946–1954, 2006. doi:[10.1152/jappphysiol.00889.2005](https://doi.org/10.1152/jappphysiol.00889.2005).
- <sup>38</sup>Stekelenburg, A., G. J. Strijkers, H. Parusel, D. L. Bader, K. Nicolay, and C. W. Oomens. Role of ischemia and deformation in the onset of compression-induced deep tissue injury: MRI-based studies in a rat model. *J. Appl. Physiol.* 102:2002–2011, 2007. doi:[10.1152/jappphysiol.01115.2006](https://doi.org/10.1152/jappphysiol.01115.2006).
- <sup>39</sup>Stockton, L., and D. Parker. Pressure relief behavior and the prevention of pressure ulcers in wheelchair users in the community. *J. Tissue Viability* 12:84–92, 2002.
- <sup>40</sup>Tam, E. W., A. F. Mak, W. N. Lam, J. H. Evans, and Y. Y. Chow. Pelvic movement and interface pressure distribution during manual wheelchair propulsion. *Arch. Phys. Med. Rehabil.* 84:1466–1472, 2003. doi:[10.1016/S0003-9993\(03\)00269-7](https://doi.org/10.1016/S0003-9993(03)00269-7).
- <sup>41</sup>Temes, W. C., and P. Harder. Pressure relief training device. *Phys. Ther.* 57:1152–1153, 1977.
- <sup>42</sup>Thomas, D. R. Prevention and treatment of pressure ulcers: what works? What doesn't? *Cleve. Clin. J. Med.* 68:704–707, 10–14, 17–22, 2001.
- <sup>43</sup>Tsokos, M., A. Heinemann, and K. Puschel. Pressure sores: epidemiology, medico-legal implications and forensic argumentation concerning causality. *Int. J. Legal Med.* 113:283–287, 2000. doi:[10.1007/s004149900125](https://doi.org/10.1007/s004149900125).
- <sup>44</sup>Verver, M. M., J. van Hoof, C. W. Oomens, J. S. Wismans, and F. P. Baaijens. A finite element model of the human buttocks for prediction of seat pressure distributions. *Comput. Met. Biomech. Biomed. Eng.* 7:193–203, 2004. doi:[10.1080/10255840410001727832](https://doi.org/10.1080/10255840410001727832).
- <sup>45</sup>Wagnac, E. L., C. E. Aubin, and J. Dansereau. A new method to generate a patient-specific finite element model of the human buttocks. *IEEE Trans. Biomed. Eng.* 55:774–783, 2008. doi:[10.1109/TBME.2007.912640](https://doi.org/10.1109/TBME.2007.912640).
- <sup>46</sup>Wey, P. D., L. A. Casas, and V. L. Lewis, Jr. Buried inferiorly based gluteus maximus musculocutaneous flap for reconstruction of large, recurrent ischiopubic pressure sores. *Ann. Plast. Surg.* 24:283–288, 1990. doi:[10.1097/0000637-199003000-00016](https://doi.org/10.1097/0000637-199003000-00016).
- <sup>47</sup>Yarnitzky, G., Z. Yizhar, and A. Gefen. Real-time subject-specific monitoring of internal deformations and stresses in the soft tissues of the foot: a new approach in gait analysis. *J. Biomech.* 39:2673–2689, 2006. doi:[10.1016/j.jbiomech.2005.08.021](https://doi.org/10.1016/j.jbiomech.2005.08.021).